

Generation of cavity-birefringence-dependent multi-wavelength bright-dark pulse pair in a figure-eight thulium-doped fiber laser

Xiao-Fa Wang(王小发), Dong-Xin Liu(刘东鑫), Hui-Hui Han(韩慧慧), Hong-Yang Mao(毛红炀)
Citation: Chin. Phys. B, 2021, 30 (**5**): 054205. DOI: 10.1088/1674-1056/abd68f
Journal homepage: http://cpb.iphy.ac.cn; http://iopscience.iop.org/cpb

What follows is a list of articles you may be interested in

Suppression of multi-pulse formation in all-polarization-maintaining figure-9 erbium-doped fiber mode-locked laser

Jun-Kai Shi(石俊凯), Deng-Feng Dong(董登峰), Ying-Ling Pan(潘映伶), Guan-Nan Li(李冠楠), Yao Li(黎尧), Li-Tuo Liu(刘立拓), Xiao-Mei Chen(陈晓梅), and Wei-Hu Zhou(周维虎)
Chin. Phys. B, 2021, 30 (**1**): 014206. DOI: 10.1088/1674-1056/abc153

Visible-light all-fiber vortex lasers based on mode selective couplers

Chuchu Dong(董楚楚), Jinhai Zou(邹金海), Hongjian Wang(王鸿健), Han Yao(尧涵), Xianglong Zeng(曾祥龙), Yikun Bu(卜轶坤), Zhengqian Luo(罗正钱)
Chin. Phys. B, 2020, 29 (**9**): 094204. DOI: 10.1088/1674-1056/aba278

Generation of single and multiple dissipative soliton in an erbium-doped fiber laser

Li-Na Duan(段利娜), Jin Wen(文进), Wei Fan(樊伟), Wei Wang(王炜)
Chin. Phys. B, 2017, 26 (**10**): 104205. DOI: 10.1088/1674-1056/26/10/104205

Nonlinear polarization rotation-induced pulse shaping in a stretched-pulse ytterbium-doped fiber laser

Bai Dong-Bi, Li Wen-Xue, Yang Kang-Wen, Shen Xu-Ling, Chen Xiu-Liang, Zeng He-Ping
Chin. Phys. B, 2014, 23 (**10**): 104208. DOI: 10.1088/1674-1056/23/10/104208

Theoretical and experimental study on all-normal-dispersion Yb-doped mode-locked fiber lasers

Chi Jun-Jie, Li Ping-Xue, Yang Chun, Zhao Zi-Qiang, Li Yao, Wang Xiong-Fei, Zhong Guo-Shun, Zhao Hong, Jiang Dong-Sheng
Chin. Phys. B, 2013, 22 (**4**): 044204. DOI: 10.1088/1674-1056/22/4/044204

Generation of cavity-birefringence-dependent multi-wavelength bright–dark pulse pair in a figure-eight thulium-doped fiber laser*

Xiao-Fa Wang(王小发)†, Dong-Xin Liu(刘东鑫), Hui-Hui Han(韩慧慧), and Hong-Yang Mao(毛红炀)

Key Laboratory of Optical Fiber Communication Technology, Chongqing Education Commission, School of Optoelectronic Engineering, Chongqing University of Posts and Telecommunications, Chongqing 400065, *China*

(Received 27 October 2020; revised manuscript received 3 December 2020; accepted manuscript online 24 December 2020)

We experimentally demonstrated a stable multi-wavelength bright–dark pulse pair in a mode-locked thulium-doped fiber laser (TDFL). The nonlinear polarization rotation (NPR) and nonlinear optical loop mirror (NOLM) were employed in a figure-eight cavity to allow for multi-wavelength mode-locking operation. By incorporating different lengths of high birefringence polarization-maintaining fiber (PMF), the fiber laser could operate stably in a multi-wavelength emission state. Compared with the absence of the PMF, the birefringence effect caused by PMF resulted in rich multi-wavelength optical spectra and better intensity symmetry and stability of the bright–dark pulse pair.

Keywords: bright–dark pulse pair, nonlinear polarization rotation, fiber laser, polarization-maintaining fiber

PACS: 42.55.Wd, 42.60.Fc, 42.65.Re, 42.25.Lc **DOI:** 10.1088/1674-1056/abd68f

1. Introduction

In the past decades, the passively mode-locked fiber lasers have attracted much attention due to their low cost, compact structure, and high stability. To date, there have been a lot of reports on mode-locked fiber lasers. By managing the parameters of the fiber resonator, different kinds of pulses, such as conventional solitons,[1] dissipative solitons,[2] vector solitons,[3,4] rectangular-shaped pulses,[5,6] chair-like pulses,[7] and h-shaped pulses[8] have been experimentally observed in passively mode-locked fiber lasers. However, the above pulses are all bright pulses. In addition to bright pulse, there is another type of pulse called dark pulse, which is also a solution of the nonlinear Schrödinger equation (NLSE).[9] It is worth noting that the dark pulse has been successively confirmed by theory[10] and experiment.[11] Dark pulse is defined as an intensity dip in the intensity of a continuous wave (CW) background of the laser emission. Compared with bright pulse, dark pulse has some advantages, such as better stability in the presence of noise, low transmission loss in fibers, and being less affected by intrapulse stimulated Raman scattering.[12] Therefore, dark pulse has great potential applications in optical communication system.

Due to the interaction between pulses, in addition to obtaining bright or dark pulses in fiber lasers, bright–bright, dark–dark, and bright–dark pulse pairs, as solutions of coupled higher-order NLSE in fiber systems,[13,14] can also be obtained. Among these, the bright–dark pulse pair exhibits wide potential applications in the fields of optical spectroscopy, optical communication, soliton evolution, and so on. It has been theoretically[15,16] and experimentally[17–25] shown that the bright pulses and dark pulses can coexist in a fiber system. In 2012, Ning *et al.* experimentally demonstrated the generation of the bright–dark pulse pair in a figure-eight dispersion-managed passively mode-locked fiber laser.[18] In 2014, Gao *et al.* demonstrated the bright–dark pulse pair in an erbium-doped fiber laser based on graphene.[20] Shortly, the bright–dark pulse pair based on Bi_2Se_3/polyvinyl alcohol in an erbium-doped ring fiber laser was reported by Guo *et al.*[21] In 2016, Zhang *et al.* reported the generation of orthogonally polarized bright–dark pulse pairs in a passively mode-locked fiber laser with a large-angle tilted fiber grating (LA-TFG).[22] In 2018, tri-wavelength bright–dark pulse pairs in a ReS_2-based mode-locked erbium-doped fiber laser were successfully obtained by Zhao *et al.*[23] Very recently, Fu *et al.* experimentally investigated the bright–dark soliton pair in an erbium-doped mode-locked fiber laser by using $Cr_2Ge_2Te_6$/polyvinyl alcohol as the saturable absorber.[24] Obviously, most of the existing reports on the bright–dark pulse pair used two-dimensional materials as mode-locking devices and focus on 1.5-μm band. Therefore, it is of great significance to expand the application of mode-locking techniques in the research of 2-μm bright–dark pulse pair.

In this paper, a multi-wavelength bright–dark pulse pair has been experimentally observed in a mode-locked TDFL. The multi-wavelength mode-locking operation of the fiber laser was achieved by employing the NPR and NOLM. By incorporating different lengths of high birefringence PMF, *i.e.*, introducing different amounts of linear cavity birefringence,

*Project supported by the National Natural Science Foundation of China (Grant No. 6170031626) and the Natural Science Foundation of Chongqing City, China (Grant Nos. cstc2018jcyjAX0585 and cstc2017zdzxX0011).

†Corresponding author. E-mail: wangxf@cqupt.edu.cn

© 2021 Chinese Physical Society and IOP Publishing Ltd

the fiber laser could operate stably in a multi-wavelength emission state. Compared with the absence of the PMF, the bright–dark pulse pair exhibited better intensity symmetry and stability after incorporating the PMF. To the best of our knowledge, it is the first time to generate multi-wavelength bright–dark pulse pair in a passively mode-locked TDFL.

2. Experimental setup

The experimental setup of the proposed TDFL is shown in Fig. 1. It consists of a right loop and a left loop, which are connected to each other by a 50:50 optical coupler (OC). In the right loop, a 6-m double-clad thulium-doped fiber (TDF, IXF-2CF-TmO-10-130, IXFiber) with absorption coefficient of 5.6 dB/m at 789 nm is used as the gain medium. Its core/inner-cladding diameters are 10 μm/125 μm corresponding to the numerical apertures (NAs) of 0.16/0.46. The TDF is pumped by a 793-nm laser diode with a max output power of 12 W through a $(2+1)\times 1$ pump combiner. A polarization-dependent isolator (PD-ISO) not only ensures unidirectional operation, but also acts as a polarizer. Two in-line polarization controllers (PCs) are employed to manipulate the cavity polarization state (PS), and they can be combined with the PD-ISO to form the NPR. The 30% port of the 70:30 OC is used for outputting laser signal from the cavity. The left loop is NOLM, which consists of a segment of twisted $\sim$ 256-m single mode fiber (SMF28e) and different lengths of PMF with birefringence of $\sim 3.5\times 10^{-4}$. When the NOLM works in intensity-dependent loss state, it can effectively suppress the mode competition caused by the homogeneous gain broadening of the TDF at room temperature to achieve stable multi-wavelength emission.[26] The total cavity length is $\sim$ 274 m, including 6-m TDF, $\sim$ 256-m SMF28e, and $\sim$ 12-m pigtail fibers of all optical components. The output characteristics of the TDFL are monitored by an optical spectrum analyzer (Omni-λ 750i, Zolix) with a resolution of 0.05 nm, a 1-GHz oscilloscope (WaveRunner 610Zi, Lecroy), and a radio-frequency (RF) spectrum analyzer (FSL3, Rohde & Schwarz) with 3-GHz bandwidth. In addition, both the oscilloscope and RF spectrum analyzer should be used together with an InGaAs photodetector (ET-5000F, EOT).

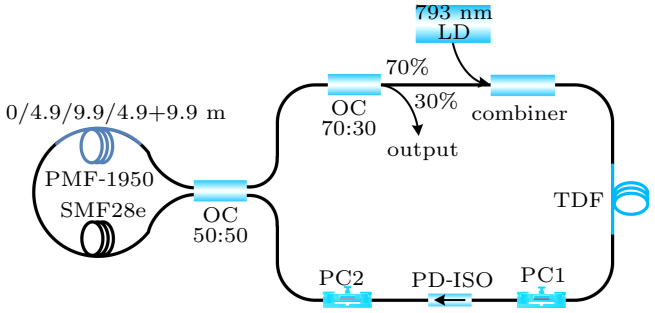


Fig. 1. Experimental setup of the mode-locked TDFL.

3. Experimental results and discussion

The average output power of the TDFL was firstly studied by changing the pump power in a wide range. As shown in Fig. 2, the threshold for oscillation and slope efficiency were found to be 2.2 W and $\sim$ 0.45%, respectively. The low slope efficiency of the TDFL is caused mainly by mode field mismatch between the double-clad TDF and the SMF28e. With the increasing of pump power, the average output power of the TDFL increases approximately linearly. As the pump power reached the oscillation threshold, the TDFL operated in two states including CW (2.2 W–3.4 W) and mode-locking (3.4 W–7 W). The maximum output power of the pump source is 12 W, but in order to protect the PD-ISO, we limited the maximum output power of the pump source to 7 W.

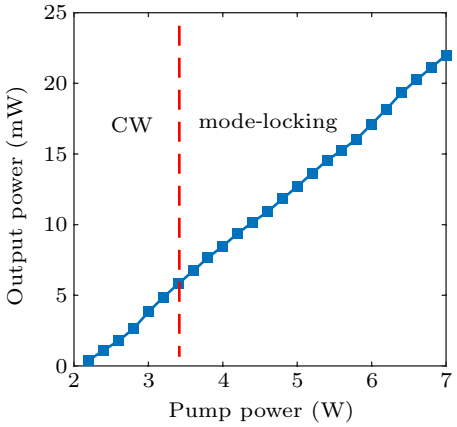


Fig. 2. Average output power under different pump powers.

3.1. TDFL without PMF

The output characteristics of the TDFL without PMF in the cavity were observed. A series of experiments show that the stable single bright–dark pulse pair could be easily obtained by adjusting the PCs carefully. Figures 3(a1)–3(c1) show the output characteristics of the TDFL in PS1 with a pump power of 7 W. The pulse train of the single bright–dark pulse pair is shown in Fig. 3(a1). The period of the pulse train is 1.34 μs, which matches with the cavity round-trip time, thus verifies the mode-locking operation of the TDFL.[27] The inset of Fig. 3(a1) shows the pulse profile of the bright–dark pulse pair. Clearly, for the bright pulse and dark pulse, they show an asymmetric profile with different pulse intensities. The optical spectrum of the mode-locked TDFL is shown in Fig. 3(b1). It can be found that the central wavelength and the full width at half maximum (FWHM) are 2010.5 nm and 12.65 nm, respectively. In addition, there exists no obvious Kelly sideband in the optical spectrum, which may be caused by the birefringent filtering effect in the cavity.[28] To investigate the stability of the bright–dark pulse pair, the RF spectrum has been measured with a resolution bandwidth (RBW) of 300 Hz and a span range of 0.6 MHz, as shown in Fig. 3(c1). The fundamental RF

peak is located at 746 kHz, corresponding to the total cavity length of ∼ 274 m. The inset of Fig. 3(c1) shows the wideband RF spectrum. The signal-to-noise ratio (SNR) of 39 dB and the wideband RF spectrum indicate good mode-locking stability. In addition, with the PCs and pump power unchanged, we have measured the stability of the spectra within four hours, and the results show that the spectra present good stability.

When the pump power was fixed at 7 W, the dual bright–dark pulse pairs could be easily obtained by further adjusting the PCs. Figures 3(a2)–3(c2) show the output characteristics of the TDFL in PS2. From the pulse train shown in Fig. 3(a2), we can see that the pulse interval remains at 1.34 μs. Compared with the single bright–dark pulse pair, the dual bright–dark pulse pairs have two bright–dark pulse pairs with similar profile in one period, as shown in the inset of Fig. 3(a2). The formation mechanism of the dual bright–dark pulse pairs may be due to the peak power clamping effect of the cavity.[29] Figure 3(b2) shows the optical spectrum of the dual bright–dark pulse pairs operation. It can be found that the central wavelength is 2010.6 nm, and the FWHM is increased to 14.35 nm. At the same time, the SNR of 40 dB and the wideband RF spectrum show that the fiber laser was working in a stable mode-locking state, as shown in Fig. 3(c2).

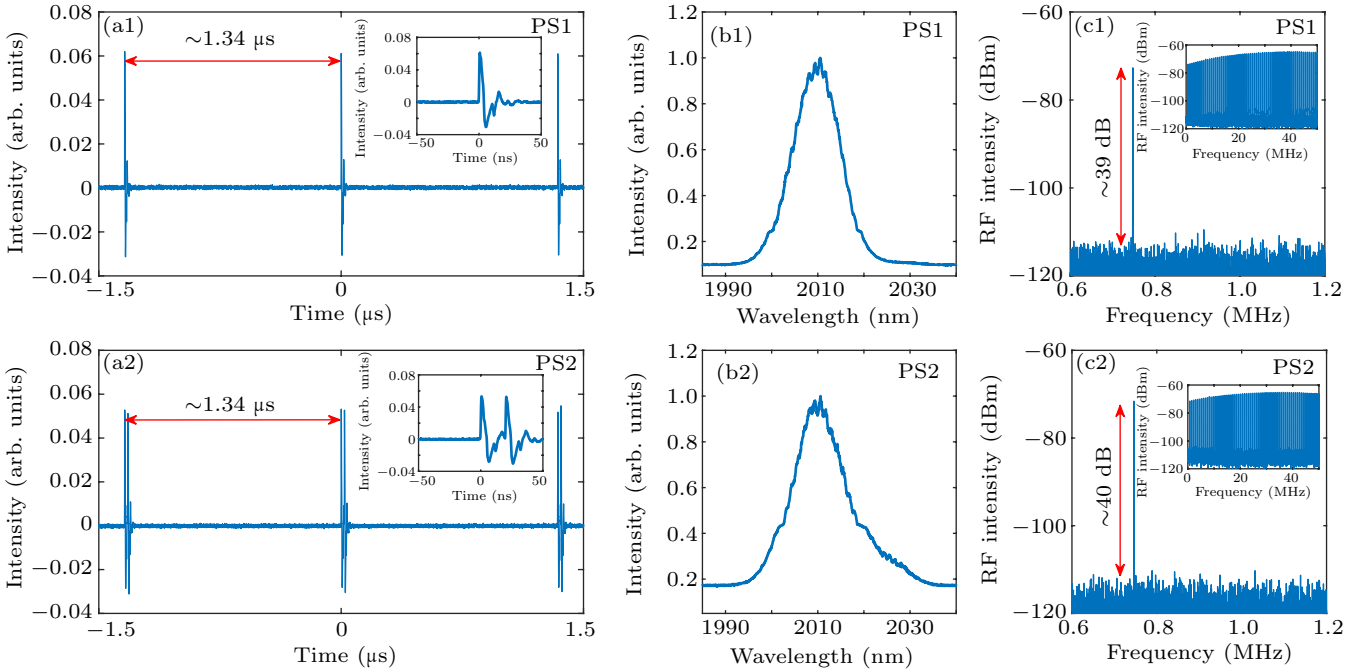


Fig. 3. Output characteristics of the TDFL in different polarization states: (a1), (a2) pulse trains (inset: the corresponding pulse profiles); (b1), (b2) optical spectra, and (c1), (c2) RF spectra at fundamental repetition rate (inset: the corresponding wideband RF spectra with a span range of 50 MHz).

3.2. TDFL with different lengths of PMF

In order to study the effect of birefringence on the transmission of the bright–dark pulse pair, different lengths of PMF were introduced into the cavity. While keeping the total cavity length constant, 4.9-m PMF, 9.9-m PMF and a piece of fiber composed of 4.9-m and 9.9-m PMF were introduced into the cavity, respectively. Figure 4 shows the output characteristics of the TDFL with different lengths of PMF at a pump power of 7 W.

Figures 4(a1)–4(a3) show the pulse profiles with different lengths of PMF in the cavity. It can be seen that three types of bright–dark pulse pairs have similar profiles and intensities. This means that different lengths of PMF may have little effect on the intensity of the dark pulse. Compared with Fig. 3(a1), the intensity of the dark pulse is greater and close to the bright pulse after incorporating the PMF. It shows that strong birefringence may be beneficial to the transmission of dark pulse. In addition, the base of the bright pulse profile became wider when the PMF was introduced into the cavity, which is similar to the Ref. [8].

As we all know, the combination of PMF, PD-ISO, and PCs is equivalent to a comb filter.[30] Therefore, the output optical spectra of the fiber laser present multi-wavelength states as shown in Figs. 4(b1)–4(b3). In Figs. 4(b1) and 4(b2), the wavelength spacings between adjacent peaks $\Delta\lambda$ are 2.3 nm and 1 nm, respectively, which can be verified by the formula[31]

$$\Delta\lambda = \lambda^2/\Delta nL, \tag{1}$$

where Δn is the birefringence of PMF, L is the length of PMF, and λ is the center wavelength of the optical spectrum. Thus, there are 12 and 33 wavelengths within the FWHM in Figs. 4(b1) and 4(b2), respectively. Interestingly, the optical spectrum shown in Fig. 4(b2) shows an M-shaped profile, which is similar to Ref. [21], implying that the formation of

the pulse may be related to the gain competition and the cavity feedback. The optical spectrum shown in Fig. 4(b3) shows irregular modulation. This may be due to the fact that the 4.9-m PMF and the 9.9-m PMF are not directly fused together, but through a piece of SMF28e. Therefore, there is an angle between the axes of two pieces of PMF. And the transmission spectrum of the comb filter becomes inhomogeneous, resulting in irregular modulation of the optical spectrum.[32]

In order to evaluate the stability of the fiber laser, the RF spectrum was measured by an RF spectrum analyzer with an RBW of 300 Hz and a span range of 0.6 MHz. These results are presented in Figs. 4(c1)–4(c3), corresponding to three different lengths of PMF in the cavity, respectively. The SNRs at the fundamental repetition rate are 41 dB, 40 dB, and 39 dB, respectively. Meanwhile, the insets of Figs. 4(c1)–4(c3) show the wideband RF spectra with a span range of 50 MHz. The wideband RF spectra have no frequency components other than the fundamental and harmonic frequencies. Compared with Ref. [24], the above results show a better stability of the bright–dark pulse pair in the TDFL.

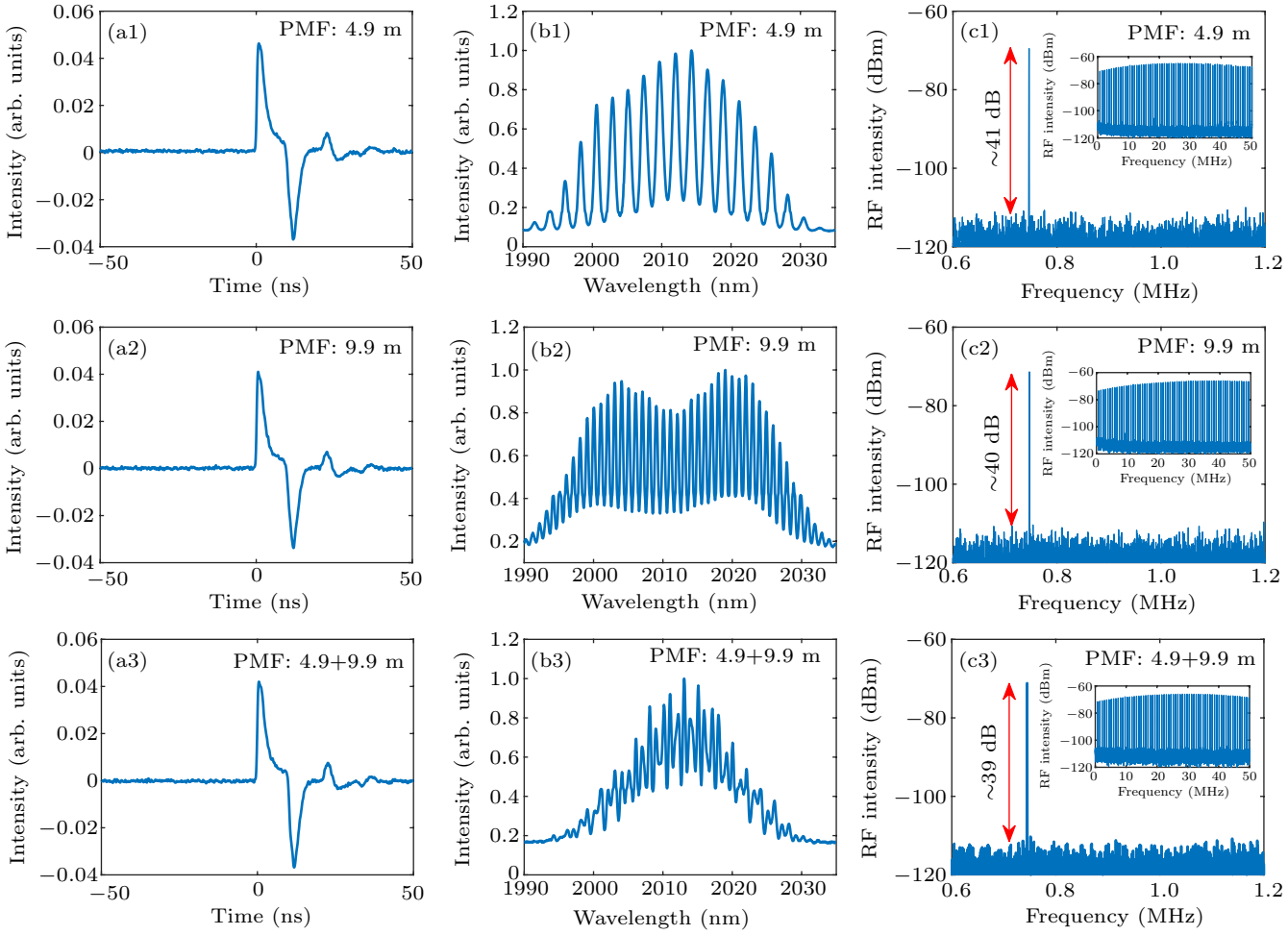


Fig. 4. Output characteristics of the TDFL with different lengths of PMF: (a1)–(a3) pulse profiles; (b1)–(b3) optical spectra, and (c1)–(c3) RF spectra at fundamental repetition rate (inset: the corresponding RF spectra with a span range of 50 MHz).

4. Conclusion

In summary, we have experimentally observed a multi-wavelength bright–dark pulse pair in a mode-locked TDFL. The NPR and NOLM were employed in a figure-eight cavity to allow for multi-wavelength mode-locking operation. We have investigated the relationship between the output characteristics of the fiber laser and the cavity birefringence by incorporating different lengths of PMF. Experimental results show that the high birefringence of the PMF is beneficial to the transmission of the dark pulse as well as the excitation of rich optical spectra. In future work, we will focus on improving the efficiency of the fiber laser and further explore the transmission and interaction mechanisms of the bright–dark pulse pair.

References

[1] Wang X F, Zhang J H, Peng X L and Mao X F 2018 *Chin. Phys. B* **27** 084215

[2] Huang S S, Wang Y G, Yan P G, Zhao J Q, Li H Q and Lin R Y 2014 *Opt. Express* **22** 11417

[3] Tang D Y, Zhang H, Zhao L M and Wu X 2008 *Phys. Rev. Lett.* **101** 153904

[4] Song Y F, Chen S, Zhang Q, Li L, Zhao L M, Zhang H and Tang D Y 2016 *Opt. Express* **24** 25933

[5] Guo B, Yao Y, Yang Y F, Yuan Y J, Jin L, Yan B and Zhang J Y 2015 *Photon. Res.* **3** 94
[6] Krzempek K and Abramski K 2016 *Opt. Express* **24** 22379
[7] Gupta P K, Singh C P, Singh A, Sharma S K, Mukhopadhyay P K and Bindra K S 2016 *Appl. Opt.* **55** 9961
[8] Zhao J Q, Li L, Zhao L M, Tang D Y and Shen D Y 2018 *Opt. Lett.* **43** 247
[9] Markom A M, Tan S J, Haris H, Paul M C, Dhar A, Das S and Harun S W 2018 *Chin. Phys. Lett.* **35** 024203
[10] Tomlinson W J, Hawkins R J, Weiner A M, Heritage J P and Thurston R N 1989 *J. Opt. Soc. Am. B* **6** 329
[11] Zhang H, Tang D Y, Zhao L M and Wu X 2009 *Phys. Rev. A* **80** 045803
[12] Song Y F, Shi X J, Wu C F, Tang D Y and Zhang H 2019 *Appl. Phys. Rev.* **6** 021313
[13] Dreischuh A, Neshev D N, Petersen D E, Bang O and Krolikowski W 2006 *Phys. Rev. Lett.* **96** 043901
[14] Tian J P, Tian H P, Li Z H and Zhou G S 2004 *J. Opt. Soc. Am. B* **21** 1908
[15] Afanasjev V V, Dianov E M and Serkin V N 1989 *IEEE J. Quantum Electron.* **25** 2656
[16] Lisak M, Höök A and Anderson D 1990 *J. Opt. Soc. Am. B* **7** 810
[17] Wang H Y, Xu W C, Cao W J, Wang L Y and Dong J L 2012 *Laser Phys.* **22** 282
[18] Ning Q Y, Wang S K, Luo A P, Lin Z B, Luo Z C and Xu W C 2012 *IEEE Photon. J.* **4** 1647
[19] Li X L, Zhang S M, Meng Y C and Hao Y P 2013 *Opt. Express* **21** 8409
[20] Gao J, Hu F M, Huo X D and Gao P 2014 *Laser Phys.* **24** 085104
[21] Guo B, Yao Y, Tian J J, Zhao Y F, Liu S, Li M and Quan M R 2015 *IEEE Photon. Technol. Lett.* **27** 701
[22] Zhang Z X, Mou C B, Yan Z J, Sun Z Y and Zhang L 2016 *Appl. Phys. B* **122** 161
[23] Zhao R W, Li G R, Zhang B T and He J L 2018 *Opt. Express* **26** 5819
[24] Fu S G, Shang X X, Zhang F, Xing F, Man Z S, Zhang W F, Wang B Y, Li D W and Zhang H N 2019 *Appl. Opt.* **58** 9217
[25] Zheng Y, Wang M X, Zhao R, Zhang H N, Liu D H and Li D W 2020 *Appl. Opt.* **59** 396
[26] Yan Z Y, Li X H, Tang Y L, Shum P P, Yu X, Zhang Y and Wang Q J 2015 *Opt. Express* **23** 4369
[27] Wang X F, Peng X L, Jiang Q X, Gu X H, Zhang J H, Mao X F and Yuan S Z 2017 *Chin. Phys. B* **26** 114205
[28] Guo B, Yao Y, Yang Y F, Yuan Y J, Wang R L, Wang S G, Ren Z H and Yan B 2015 *J. Appl. Phys.* **117** 063108
[29] Tang D Y, Zhao L M, Zhao B and Liu A Q 2005 *Phys. Rev. A* **72** 043816
[30] Liu S, Yan F P, Ting F, Zhang L N, Bai Z Y, Han W G and Zhou H 2016 *IEEE Photon. Technol. Lett.* **28** 864
[31] Ma W Z, Wang T S, Wang F R, Zhao D S, Liu R M, Zhang J and Jiang H L 2019 *IEEE Photon. Technol. Lett.* **31** 242
[32] Liu J W, Tong Z R, Zhang W H, Shi X T and Li J X 2020 *Laser Phys.* **30** 115101